Chemical Science

ROYAL SOCIETY OF CHEMISTRY

EDGE ARTICLE

View Article Online
View Journal | View Issue

Cite this: *Chem. Sci.*, 2026, **17**, 8976

All publication charges for this article have been paid for by the Royal Society of Chemistry

Received 5th January 2026
Accepted 8th March 2026

DOI: 10.1039/d6sc00062b

rsc.li/chemical-science

Single-position ligand modifications tune CB_2R activity by targeting the toggle switch

Rudolf L. Z. Ganzoni, †[a] Miroslav Kosar, †[a] Yongqi Han, [b] Rosa Maria Vitale, [c] Pietro Amodeo, [c] Xiaoting Li, [d] Zhonghua Zha, [d] Kacper J. Patej, [a] Bilal Kicin, [a] Taddäus E. N. Strunden, [a] Lisa Reichert, [a] Uxía Gómez-Bouzó, [a] Themiya P. Perera, [b] Kenneth Atz, [e] Wolfgang Guba, [e] Christian Bartelmus, [e] Raphael Bigler, [f] Paolo Tosatti,[f] Stephan Bachmann,[f] Tian Hua, [d] David A. Sykes, *[b] Dmitry B. Veprintsev, *[b] Uwe Grether *[e] and Erick M. Carreira *[a]

Cannabinoid receptor type 2 (CB_2R) is a prominent class A G protein-coupled receptor (GPCR) and is a therapeutic target of interest for inflammatory diseases, pain management, and neurodegenerative disorders. We report the development of ligands based on HU-308 that share a single central scaffold but bear diverse sidechains, enabling controlled modulation of GPCR activation. Structural modifications at a single position of the parent ligand allow modulation of the single-residue toggle switch of CB_2R, Trp258$^{6.48}$, and thereby control over receptor activity. A continuum of functional outcomes is achieved through interaction of the ligands with the CB_2R toggle switch, leading to full agonism, partial agonism, neutral antagonism, or partial inverse agonism. Several low-efficacy ligands display protean behavior across assays, underscoring context-dependent modulation of CB_2R and its importance in profiling such ligands. A notable compound within this series is CF_3-substituted (*S*)-**1**, which displays distinct CB_2R affinity, potency, and a biased CB_2R signaling profile. We provide a rationale based on molecular dynamics simulations for the unique pharmacological profile observed and suggest that stabilization of an active receptor conformation occurs by close-contact interaction of (*S*)-**1** with the CB_2R toggle switch. Our findings demonstrate that strategic structural modifications of class A GPCR ligands may, by targeting a receptor's toggle switch, shift ligands to different positions along the efficacy spectrum, independent of their parent scaffold's original functional profile.

Introduction

G protein-coupled receptors (GPCRs) represent the largest family of membrane proteins in the human genome and are targets for approximately one-third of all approved drugs by the Food and Drug Administration (FDA),[1,2] with class A GPCR subpopulations constituting approximately 86% of GPCR drug targets.[3] Class A GPCRs have attracted substantial interest and investment,[3–5] with the market for small-molecule modulators projected to grow significantly in the coming years.[6] However, the challenge associated with discovering new ligands for a target is significant,[7] and developing suitable leads into a drug is underscored by its prohibitive cost.[8–10] The process of lead identification for GPCR targets is particularly difficult because of a variety of different binding and activation modes and the associated, diverse functional outcomes at the receptor.[7,11]

The cannabinoid receptors are prominent examples of class A GPCRs which hold promise for treatment of various ailments[12] but have fallen short of that promise so far.[13] In recent years, cannabinoid receptor 2 (CB_2R) especially has garnered significant interest as a therapeutic target. As CB_2R is mainly expressed in immune cells in the periphery,[14,15] selective pharmacological intervention at CB_2R offers potential for the treatment of neuroinflammation,[16] autoimmune disorders,[17,18] chronic pain,[19,20] as well as cancer[21,22] while circumventing adverse effects associated with cannabinoid receptor 1 (CB_1R)

[a]*Laboratorium für Organische Chemie, Eidgenössische Technische Hochschule Zürich, Vladimir-Prelog-Weg 3, 8093 Zürich, Switzerland. E-mail: erickm.carreira@org.chem.ethz.ch*

[b]*Faculty of Medicine & Health Sciences, University of Nottingham, Centre of Membrane Proteins and Receptors (COMPARE), Nottingham NG7 2UH, UK. E-mail: david.sykes@nottingham.ac.uk; dmitry.veprintsev@nottingham.ac.uk*

[c]*Institute of Biomolecular Chemistry, National Research Council, Via Campi Flegrei 34, 80078 Pozzuoli, Italy*

[d]*iHuman Institute, ShanghaiTech University, Shanghai 201210, China*

[e]*Roche Pharma Research & Early Development, Roche Innovation Center Basel, F. Hoffmann-La Roche Ltd, 4070 Basel, Switzerland. E-mail: uwe.grether@roche.com*

[f]*Department of Process Chemistry and Catalysis, F. Hoffmann-La Roche Ltd, Basel 4070, Switzerland*

† Rudolf L. Z. Ganzoni and Miroslav Kosar contributed equally to this work and therefore share co-first authorship.

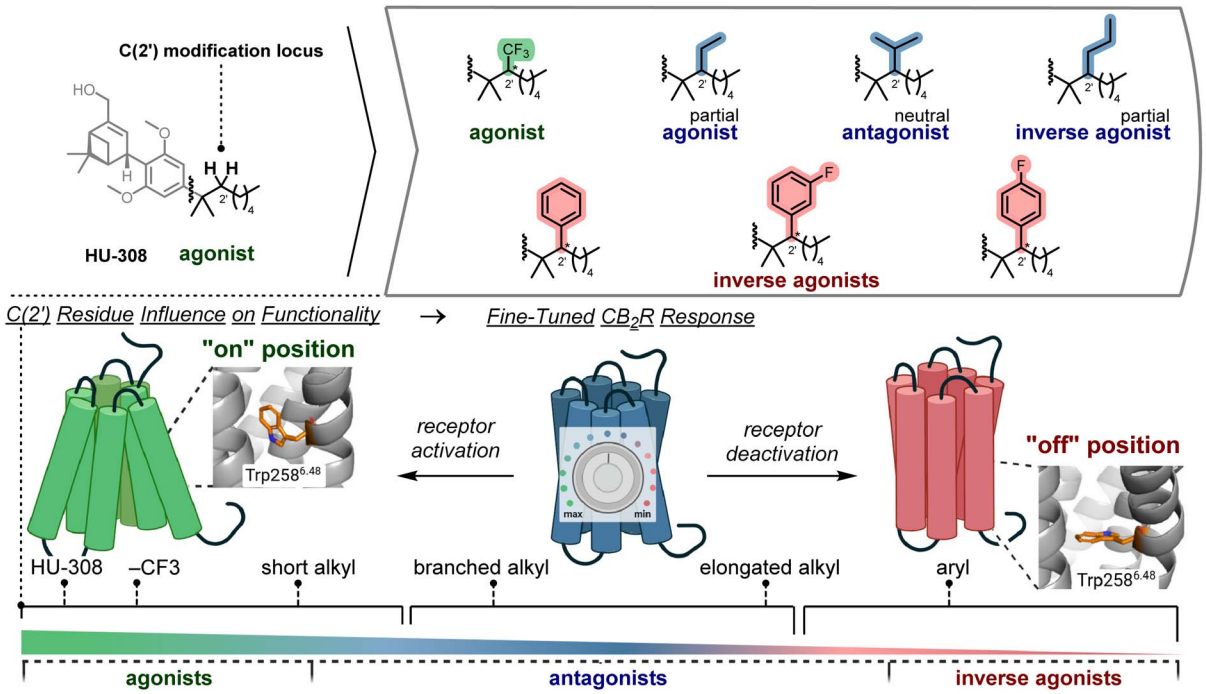

Fig. 1 Ligand design based on the HU-308 scaffold and modification of the C(2′) position. Fine-tuned actuation of the CB_2R Trp258$^{6.48}$ single-residue toggle switch leads to a continuum of functional outcomes at the receptor.[29]

modulation.[23] The promising therapeutic potential of selective CB_2R modulation, however, has not yet successfully translated to the clinic,[24,25] with recent discontinuation of development programs aimed at treatment of cancer[26] and irritable bowel syndrome.[27] Most recently, development of ajulemic acid (Lenabasum), a CB_1R/CB_2R dual agonist for the treatment of cystic fibrosis and dermatomyositis, was discontinued as of 2023.[28]

The apparent difficulty of advancing CB_2R selective compounds in the clinic underpins the need for a better understanding of structural determinants of receptor activation. Indeed, there is a paucity of fine-tunable ligands to activate or deactivate CB_2R over the entirety of its efficacy spectrum: agonists ↔ partial agonists ↔ neutral antagonists ↔ inverse agonists.

Despite the abundance of known CB_2R agonists, CB_2R-selective partial agonists are scarce.[30–32] This scarcity reflects the challenges in designing ligands that finely tune receptor activity without inducing maximal activation or complete inhibition. Receptor density and coupling efficiency are two key factors known to influence the apparent degree of agonism.[33,34] Consequently, the pharmacological behavior of partial agonists is highly context dependent: the same ligand may function as an agonist, neutral antagonist, or inverse agonist, depending on basal activity and cellular environment in native as well as overexpressing systems. In this respect, context dependence of ligand efficacy has been referred to as protean agonism. For example, as described in pioneering studies, in systems with high constitutive CB_2R activity, low-efficacy partial agonists (AM-1241 and L768242) may function as neutral antagonists or inverse agonists, whereas in systems with reduced basal activity, the same ligands can activate the receptor.[35]

In the clinic, it has been suggested that partial agonists may offer better control of context-dependent modulation, thereby achieving desired therapeutic effects.[4,36,37] For example, Δ^9-tetrahydrocannabinol (THC), a CB_1R/CB_2R partial agonist, elicits milder psychotropic adverse effects compared to synthetic compounds known to be full agonists of CB_1R (*e.g.* CP-55940, HU-210).[38,39] In the context of CB_2R, the partial CB_2R-selective agonist LEI-102 was shown to effectively protect against cisplatin induced kidney injury in mice.[40] This finding is particularly relevant given that CB_2R activation by full agonists has negative implications for immunosuppression, leading to infection and sepsis.[41,42] Analogously, limited downmodulation by partial inverse agonists may offer opportunities in ameliorating conditions which result from increased basal tone, without completely abolishing signaling and thereby disrupting the receptor's role in maintaining homeostasis.[43,44]

Previous work from our group focused on fluorescent imaging of CB_2R.[45] We detailed a C(2′) phenyl-substituted HU-308 (ref. 46) derivative that displayed inverse agonist activity. Notably, the ligand retains its inverse agonist functional profile, affinity, and selectivity independent of its conjugation to a range of fluorescent reporters (*e.g.* DY-480XL, fluorescein, Alexa488). We wondered whether variation of substituents at C(2′) (Fig. 1) would offer a venue for a novel approach to ligand design that leverages reutilization of known scaffolds for the purpose of covering a broader and fine-tuned range of accessible functionality.

Herein, we provide a basis for strategic structural alterations at an established class A GPCR ligand to venture beyond switch-like, binary functional responses. Inspired by recent reports showcasing intermediate receptor states of class A GPCRs that populate an active-to-inactive continuum,[47] we sought to elicit gradual functional outcomes at CB_2R. It has recently been appreciated that the activity of many class A GPCRs hinges on conformational flexibility of residues within the receptor that function as molecular toggle switches.[2,48] Targeting the precise modulation of a receptor's toggle switch therefore presents an opportunity to access its efficacy spectrum and elicit fine-tuned functional responses. In this respect, we employ a single, exemplary molecular scaffold to elicit functional outcomes spanning the efficacy spectrum of the receptor by virtue of targeted modulation of Tryptophan $258^{6.48}$ ($Trp258^{6.48}$), the single-residue toggle switch of CB_2R.[40,49,50]

Based on the canonical CB_2R ligand HU-308 (ref. 46) and intuitive design principles guided by docking studies, we synthesized and studied a collection of CB_2R ligands. The ligands we describe display high CB_2R affinity and excellent selectivity for CB_2R over CB_1R. Profiling in a panel of *in vitro* (G protein recruitment) as well as *in cellulo* (cyclic adenosine monophosphate (cAMP) production, β-arrestin recruitment, G protein recruitment) functional assays revealed a spectrum of accessible ligand efficacy compared to its parent scaffold spanning agonist, partial agonist, neutral antagonist, and inverse agonist functionality. The assays were benchmarked with canonical balanced agonist CP-55,940 (ref. 51–53) and CB_2R-selective inverse agonist SR-144,528.[51] An exemplary compound within the series synthesized, C(2′) CF_3-derivative (*S*)-**1**, a high-affinity partial agonist, was investigated by molecular dynamics (MD) simulations. This revealed a close contact interaction between (*S*)-**1** and $Trp258^{6.48}$ in the CB_2R/ligand complex.

Results and discussion

In silico ligand design

Our studies were based on the hypothesis that varying substituent size at the C(2′) position of the HU-308-derived ligands would affect the functional outcome at the receptor. At the onset of our investigation, we conducted docking studies to rapidly evaluate the influence of various substitutions at the homobenzylic C(2′) position of the HU-308 sidechain. This approach was aimed at qualitatively assessing the potential to modulate the $Trp258^{6.48}$ toggle switch by employing a simple-to-use model based on substituent size and to provide an initial gauge of the hypothesis' viability (Fig. 2, see SI). We focused on HU-308 derivatives where substitution at the C(2′) position would incrementally alter the steric bulk in the binding pocket and thereby affect the fit of these molecules in either the active or inactive state of CB_2R. We sought to explore the extent to which larger or modified aryl groups could be accommodated in the cleft hosting the CB_2R toggle switch and to assess their potential to elicit a more efficacious inverse agonist response. Accordingly, we expected smaller substituents to exhibit partial

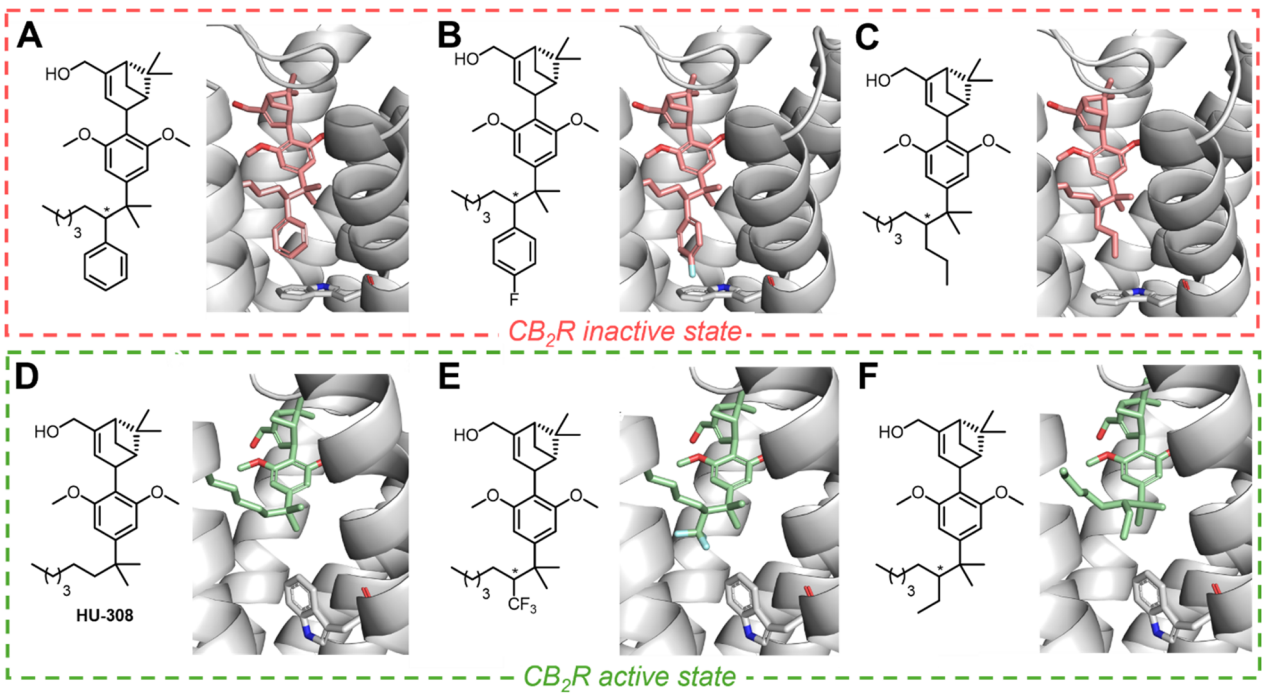

Fig. 2 Docking studies of a representative panel of candidate molecules (A) phenyl (light red), (B) *p*-F-phenyl (light red), and (C) *n*-propyl (light red)-substituted HU-308 derivatives docked into the inactive state of the receptor (PDB: 5ZTY), displaying no major steric clashes. (D) HU-308 parent compound (mint green), (E) CF_3-substituted derivative (mint green), and (F) ethyl (mint green)-substituted HU-308 derivatives only fit the active state of CB_2R (PDB: 8GUS). Protein backbone atoms are represented as ribbons colored in light gray. Nitrogen and oxygen are colored blue and red, respectively.

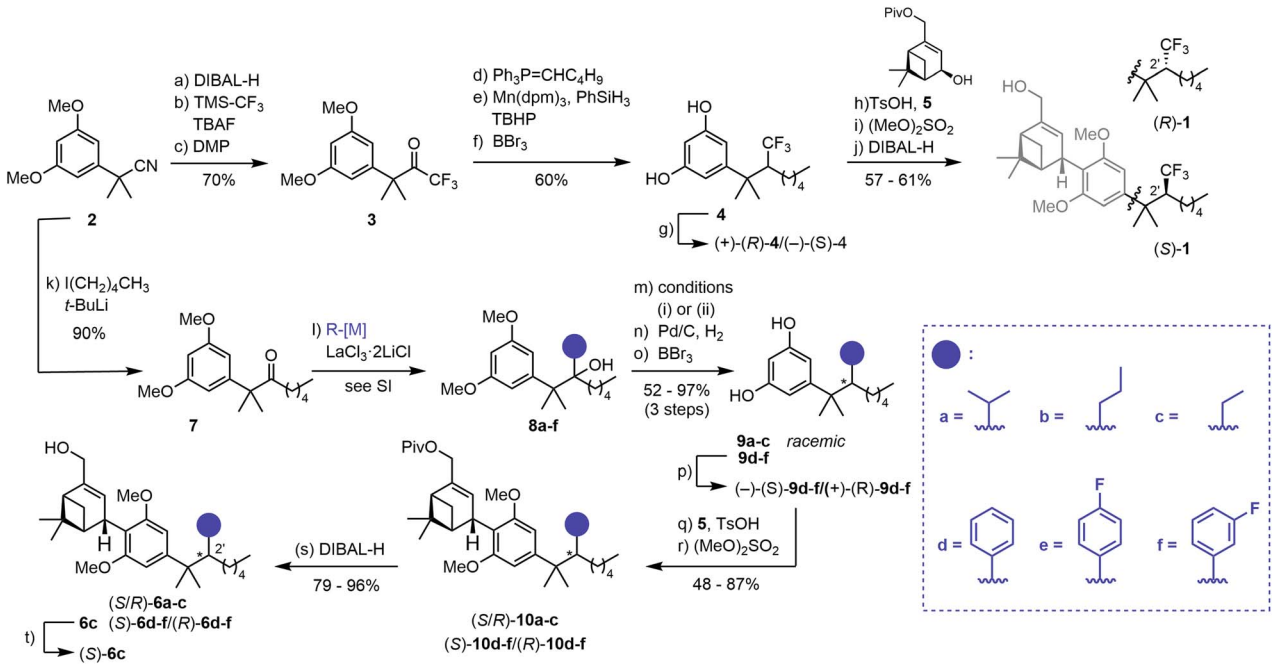

Scheme 1 Synthesis of HU-308-derived C(2′)-substituted CB_2R ligands. (a) DIBAL-H, CH_2Cl_2, −78 °C to rt, 96%; (b) TMS-CF_3, TBAF, −78 °C to rt, 94%; (c) DMP, CH_2Cl_2, 0 °C to rt, 78%; (d) $Ph_3P(C_5H_{11})Br$, *n*-BuLi, −78 °C to rt, 73%; (e) $Mn(dpm)_3$, $PhSiH_3$, TBHP, *i*-PrOH, 83%; (f) BBr_3, CH_2Cl_2, 0 °C to rt, 99%; (g) semi-preparative SFC, see SI for details; (h) TsOH·H_2O, **5**, CH_2Cl_2, 74–78%; (i) $(MeO)_2SO_2$, K_2CO_3, acetone, 94–97%; (j) DIBAL-H, CH_2Cl_2, 0 °C, 81–82%; (k) $I(CH_2)_4CH_3$, *t*-BuLi, Et_2O, pentane, −78 °C to rt, 90%; (l) R-[M], $LaCl_3$·LiCl, THF, 0 °C, 71–99%, see SI for details; (m) (i) KHMDS, CS_2, MeI, THF, −78 °C to rt, then 40 °C, or (ii) $SOCl_2$, DMAP, pyridine, 0 °C to rt, see SI for details; (n) Pd/C, H_2 (7–75 atm); (o) BBr_3, CH_2Cl_2, 0 °C, 52–97% over 3 steps; (p) semi-preparative SFC, see SI for details; (q) TsOH·H_2O, **5**, CH_2Cl_2; (r) $(MeO)_2SO_2$, K_2CO_3, acetone, 48–87% over 2 steps; (s) DIBAL-H, CH_2Cl_2, 0 °C, 79–96%; (t) semi-preparative SFC, see SI for details.

agonist or neutral antagonist activity, as they could be accommodated by both the active and inactive receptor states.

The docking studies indicated that even moderately more spatially demanding groups than phenyl at C(2′), such as benzyl, would exceed the limits of the binding pocket (in both the active and the inactive receptor state) and likely diminish affinity for the receptor. Consequently, phenyl and *para*/*meta*-fluorine-substituted phenyl groups were selected as possessing maximal substituent volume likely to maintain a favorable fit, as judged by computational modeling (Fig. 2A and B). Our qualitative docking studies suggested that aryl modifications, as well as C(2′) *n*-propyl substitution (Fig. 2C) could be accommodated only within the inactive state of CB_2R, whereas smaller aliphatic side chains were predicted to fit both the active and inactive receptor conformation (Fig. 2D–F). Based on this initial viability check, we proceeded to compile a focused panel of potential ligands.

To the best of our knowledge, the only other reported modification at the analogous C(2′) position involves the study of Δ^8-THC-derivatives with CH_3/H substitution at C(2′) and H/H substitution at C(1′), which is associated with CB_2R selectivity over CB_1R.[54] Beyond that, there is a lack of studies elucidating how small aliphatic groups at this position influence receptor affinity or what drives the compounds' functional profiles. This further motivated our investigation into rational structural modification beyond methyl at the C(2′) position of HU-308, shifting ligand functionality away from full agonism. This emerged as a working model to tune ligand functionality across a broad efficacy spectrum.

Synthesis

A modular synthetic approach was employed to access a panel of C(2′) substituted HU-308 derivatives. In the synthesis of fluorescent inverse agonist probes based on HU-308 amide derivatives, a dialkyl ketone readily underwent addition by phenyl lithium to give a tertiary alcohol that was subjected to dehydration and reduction.[45] Implementation of this strategy to access CF_3-substituted derivatives (*R*)-**1** and (*S*)-**1** failed and required a new approach. The synthesis of (*R*)-**1**/(*S*)-**1** commenced with reduction of nitrile **2** to the corresponding aldehyde, which was then treated with TMS-CF_3 (ref. 55) and tetrabutylammonium fluoride (TBAF) (Scheme 1).[56] Subsequent oxidation with Dess-Martin Periodinane (DMP) afforded CF_3-ketone **3** (70%, 3 steps). Introduction of the *n*-pentyl fragment proved problematic, as ketone reduction by the corresponding organometal reagent[57,58] occurred preferentially over 1,2-addition. However, treatment of **3** with $Ph_3P{=}CHC_4H_9$ effected efficient olefination. Attempted olefin reduction under classical hydrogenation conditions (Pd/C, H_2) proved challenging, as no conversion was observed at 1 atm, and reaction at elevated pressure (7 atm) was accompanied by week-long reaction times and overreduction of the resorcinol to the corresponding cyclohexane. Consequently, we employed a modified hydrogen atom transfer (HAT) procedure[59] to effect smooth reduction of

the unusual CF_3-olefin. Subsequent demethylation afforded resorcinol **4** in 60% yield (3 steps). Separation by semi-preparative supercritical fluid chromatography (SFC) furnished the two enantiomers (+)-(*R*)-**4** and (−)-(*S*)-**4** in excellent enantiomeric excess (ee) (>99% and 98%, respectively). The absolute configuration of the C(2′) stereocenter was unambiguously established by X-ray crystallographic studies of a derivative (see SI and Schemes S1 and S2). The parallel synthesis of (*R*)-**1**/(*S*)-**1** was completed by Friedel–Crafts allylation of (*R*)-**4** and (*S*)-**4** with allylic alcohol **5** in the presence of $TsOH \cdot H_2O$. This was followed by methylation and pivalate removal, affording the CF_3-bearing HU-308-derivatives in 57 to 61% yield over three steps.

The synthesis of a collection of HU-308 derived ligands, (*S*/*R*)-**6a–c**, (*S*)-**6c**, (*S*)-**6d–f**, and (*R*)-**6d–f** was also initiated from common nitrile precursor **2** (Scheme 1). Treatment of **2** with *n*-pentyl lithium, followed by imine hydrolysis, afforded dimethyl benzyl ketone **7**. A variety of substituents were introduced by organometal 1,2-addition mediated by $LaCl_3 \cdot 2LiCl$,[60] essential for the high efficiency of this step, providing tertiary alcohols **8a–f**. Subsequent elimination of the alcohols generated the respective olefins. Cleavage of the methyl ethers and hydrogenation mediated by Pd/C afforded resorcinols **9a–f** in good yields (52 to 97%, 3 steps). We carried out extensive efforts to develop an enantioselective hydrogenation protocol. However, the highest ee achieved was 80% (see SI, Table S1). Separation of **9a–f** by semi-preparative SFC proved effective for isolation of enantiomers (−)- and (+)-**9d–f** (98–>99% ee). The assignment of the absolute configuration of (−)-(*S*)-**9d** and (+)-(*R*)-**9d** was carried out by independent synthesis from a previously characterized compound[45] (see SI). For (−)-(*S*)-**9e**/(+)-(*R*)-**9e** and (−)-(*S*)-**9f**/(+)-(*R*)-**9f** the configuration is assigned by analogy based on SFC retention times and optical rotation (see SI).

Attempts at separation of the enantiomers for **9a–c** were not met with success. More than 20 chiral SFC columns were screened, and separation was attempted at multiple synthetic stages. However, efforts to resolve the enantiomers were mostly unsuccessful. To nevertheless assess the influence of these intermediate-size C(2′) sidechains, **9a–c** were then employed as racemates, affording inseparable C(2′) diastereomer mixtures in the subsequent steps. With resorcinols (−)-(*S*)-**9d–f**, (+)-(*R*)-**9d–f** and **9a–c** in hand, we set our sights on the completion of the synthesis in analogy to (*R*)-**1**/(*S*)-**1**: Friedel–Crafts allylation with **5** proceeded smoothly and furnished, after methylation, pivalates (*S*)-**10d–f**, (*R*)-**10d–f**, and (*S*/*R*)-**10a–c** in good yields (48 to 87%, 2 steps). In a last step, reductive cleavage of the pivalate afforded HU-308 analogs (*S*)-**6d–f**, (*R*)-**6d–f**, and (*S*/*R*)-**6a–c** (79 to 96%). At this stage, one diastereomer of **6c** could be separated by semi-preparative SFC, affording (+)-**6c** (99% ee), whose configuration was tentatively assigned as (*S*) by analogy to (*R*)-**1**/(*S*)-**1** (see SI).

Affinity profiling: competition binding assay

To validate that the HU-308 derivatives synthesized interact with CB_2R and retain the high selectivity of the parent compound, we determined their binding affinities at CB_2R and CB_1R. To that end, we employed our validated time-resolved Förster resonance energy transfer (TR-FRET) binding assay.[45,61–64] HEK293 membrane preparations of SNAP-Lumi4-Tb labelled hCB_2R and hCB_1R were incubated with a validated fluorescent probe (see SI) and the novel ligands (Table 1).[64] In accord with our previous findings with phenyl-modified HU-308 derivatives, compounds (*S*)-**6d** and (*R*)-**6d** showed high affinity for CB_2R ($pK_i = 7.15$ and 8.88, respectively), as well as excellent selectivity for CB_2R over CB_1R in the case of (*R*)-**6d** (243-fold). Similarly, CF_3-bearing derivatives (*R*)-**1** and (*S*)-**1** displayed selectivity for CB_2R (18- and 3615-fold, respectively) with (*S*)-**1** standing out with its high affinity ($pK_i = 9.57$). In contrast, (*R*)-**1** showed attenuated CB_2R affinity ($pK_i = 6.56$). The trend of high binding affinities continued for derivatives bearing aliphatic sidechains, as apparent for (*S*/*R*)-**6a** ($pK_i = 9.87$) as well as (*S*)-**6c** and (*S*/*R*)-**6c** ($pK_i = 8.96$ and 9.76, respectively). (*S*)-**6c** Displayed six-fold reduced affinity compared to (*S*/*R*)-**6c**. (*S*/*R*)-**6b** Displayed good binding and selectivity at CB_2R ($pK_i = 8.62$, K_i ratio = 1996).

Table 1 TR-FRET-based profiling of binding affinity[a]

		pK_i [nM]		
Ligand	C(2′)-R	CB_2R	CB_1R	K_i ratio (CB_1R/CB_2R)
(*R*)-**1**	CF_3	6.56 (±0.11)	5.37 (±0.20)	18
(*S*)-**1**	CF_3	9.57 (±0.42)	5.84 (±0.30)	3615
(*S*/*R*)-**6a**[b]	*i*-Pr	9.87 (±0.21)	5.50 (±0.12)	20 912
(*S*/*R*)-**6b**[b]	*n*-Pr	8.62 (±0.18)	5.50 (±0.10)	1996
(*S*)-**6c**[c]	Et	8.96 (±0.16)	5.93 (±0.20)	1189
(*S*/*R*)-**6c**[b]	Et	9.76(±0.16)	5.75 (±0.37)	19 098
(*S*)-**6d**	Ph	7.15 (±0.07)	6.30 (±0.26)	10
(*R*)-**6d**	Ph	8.88 (±0.03)	6.66 (±0.26)	243
(*S*)-**6e**[c]	*p*-F-Ph	6.13 (±0.07)	6.36 (±0.27)	1
(*R*)-**6e**[c]	*p*-F-Ph	7.41 (±0.33)	6.27 (±0.26)	11
(*S*)-**6f**[c]	*m*-F-Ph	7.01(±0.18)	5.85 (±0.20)	15
(*R*)-**6f**[c]	*m*-F-Ph	9.12 (±0.20)	6.26 (±0.05)	600
HU-308[d]	—	7.57[d]	5.41[d]	145[d]
CP-55,940[d]	—	7.51[d]	8.32[d]	6[d]
SR-144,528[d]	—	8.55[d]	6.43[d]	131[d]

[a] Competition binding data (pK_i) were determined in a TR-FRET assay at 37 °C with membrane preparations from either hCB_2R-HEK293 or hCB_1R-HEK293 cells. Data shown as a mean, $N = 3$–4 (±SEM). [b] C(2′) Diastereomeric mixture. [c] C(2′) Configuration assigned by analogy. [d] Previously reported in the same assay.[64]

Docking studies had predicted that fluorinated phenyl side chains would be accommodated within the CB_2R binding pocket, and indeed we observed binding of these compounds at CB_2R, albeit with a slight drop in affinity. Fluoroarene derivatives (*S*)-**6e**/(*R*)-**6e** ($pK_i = 6.13$ and 7.41, respectively) and (*S*)-**6f**/(*R*)-**6f** ($pK_i = 7.01$ and 9.12, respectively) exhibited reduced binding affinities compared to their non-fluorinated counterparts (*S*)-**6d** and (*R*)-**6d**. (*R*)-**6f** retained good selectivity (600-fold) and comparable affinity ($pK_i = 9.12$) to (*R*)-**6d** for CB_2R. These findings suggest that the *para* fluorine substituents on the C(2′) phenyl sidechains introduce steric bulk that is not optimally accommodated by the pocket that harbors the single-residue toggle switch $Trp258^{6.48}$. Such substitution may lead to unfavorable interactions within the binding pocket of the receptor. A

decrease in selectivity of these fluorinated HU-308 congeners for CB_2R over CB_1R may stem from their decreased affinity for CB_2R, especially in the case of *para*-fluorination.

With binding profiles established, we next proceeded to systematically characterize the pharmacological responses elicited across established CB_2R signaling pathways. Since the parent compound HU-308 behaves as a potent full agonist at CB_2R,[46,51] we were particularly interested to examine whether we could observe fine-tuned functional outcomes differing from full agonism.

Functional profiling: cAMP production, G protein recruitment, and β-arrestin recruitment

A canonical signaling pathway of CB_2R involves its interaction with $G\alpha_{i/o}$ proteins, which transiently inhibit adenylyl cyclase, leading to a reduction in cellular cAMP levels and the suppression of protein kinase A activity.[65] Accordingly, we focused our attention on elucidating the functional profiles of the HU-308 derivatives in a homogeneous time-resolved fluorescence (HTRF) cAMP assay and a bioluminescence resonance energy transfer (BRET) G_i-CASE assay (Table 2).[66]

In the cAMP assay, the derivatives synthesized spanned a range of functionality from agonists (Table 2, *e.g.* (*S*)-**1**) to inverse agonist (Table 2, *e.g.* (*R*)-**6d**), with efficacies (E_{max}) ranging from 95 to −46%. Interestingly, both (*R*)-**1** and (*S*)-**1** displayed agonistic behavior, triggering decrease in cAMP levels, albeit with considerably differing potencies (pEC_{50} = 6.59 and 7.97, respectively).

Ethyl-substituted HU-308 derivatives (*S*)-**6c** and (*S*/*R*)-**6c** displayed partial agonist properties (E_{max} = 69% and 81%, respectively) in the assay together with high potencies (pEC_{50} = 7.36 and 6.87, respectively). HU-308 derivative (*S*/*R*)-**6a** with a branched *i*-Pr group displayed neutral antagonist behavior while elongated *n*-Pr-substituted derivative (*S*/*R*)-**6b** behaved as an inverse agonist (E_{max} = −33%). Substituents at the C(2′) position apparently mediate a fine-tuned grading of functionality from agonism to inverse agonism. These observations for the first time demonstrate the effect of relatively minor increases in sidechain size at C(2′) on the ligands' functional profiles.

Stringent size requirements to modulate CB_2R toggle switch. (*R*)-**6d** Proved a more potent inverse agonist than (*S*)-**6d** (pEC_{50} = 6.61 and 6.32, respectively). Our initial hypothesis was that increasing size of the C(2′) phenyl substituent by means of fluorine substitution would increase inverse agonist activity, however, fluorinated derivatives did not show increased inverse agonist properties. *Meta*-F-substituted derivatives (*S*)-**6f** and (*R*)-**6f** (E_{max} = −30 and −43%, respectively) displayed inverse agonist character comparable to (*S*)-**6d** and (*R*)-**6d**, while *para*-F-substituted derivatives showed attenuated inverse agonist efficacy: (*S*)-**6e** (E_{max} = −18%) displayed reduced efficacy compared to (*S*)-**6d**, and (*R*)-**6e** displayed neutral antagonist character in the cAMP assay. We suspect that *para*-F substitution resulted in a pronounced reduction in inverse agonist efficacy due to increased steric bulk of the side chain, highlighting the stringent structural requirements for modulating the CB_2R $Trp258^{6.48}$ single-residue toggle switch. These results suggest that increases in the size of the C(2′) substituent may enhance inverse agonist efficacy only up to a threshold. Sidechains exceeding the pocket's capacity lead to a decrease in the ligands' inverse agonist efficacy and potency.

Evaluation across multiple assays hint at protean agonism. Next, we investigated the compounds' effects on G protein recruitment by CB_2R. To that end, we employed our validated BRET G_i-CASE assay.[66] Membrane preparations from hCB_2R-

Table 2 Functional characterization in CB_2R HTRF cAMP[a] and CB_2R G_i-CASE assays[b]

		HTRF cAMP assay		G_i-CASE assay	
Ligand	C(2′)-R	pEC_{50}	E_{max}/%	pEC_{50}	E_{max}/%
(*R*)-**1**	CF_3	6.59 (±0.12)	90 (±6)	6.48 (±0.13)	62 (±10)
(*S*)-**1**	CF_3	7.97 (±0.09)	95 (±4)	9.42 (±0.19)	78 (±1)
(*S*/*R*)-**6a**[e]	*i*-Pr	—	—	8.31 (±0.20)	40 (±4)
(*S*/*R*)-**6b**[e]	*n*-Pr	7.01 (±0.23)[c]	−33 (±5) [−45 (±7)][d]	7.15 (±0.03)	24 (±6)
(*S*)-**6c**[f]	Et	7.36 (±0.15)	69 (±6)	8.2 (±0.19)	80 (±17)
(*S*/*R*)-**6c**[e]	Et	6.87 (±0.11)	81 (±5)	8.72 (±0.25)	67 (±5)
(*S*)-**6d**	Ph	6.32 (±0.25)[c]	−25 (±4) [−34 (±5)][d]	8.29 (±0.22)[c]	−28 (±8) [−41 (±12)][d]
(*R*)-**6d**	Ph	6.61 (±0.17)[c]	−46 (±5) [−63 (±7)][d]	8.47 (±0.12)[c]	−43 (±9) [−64 (±13)][d]
(*S*)-**6e**[f]	*p*-F-Ph	5.66 (±0.31)[c]	−18 (±5) [−25 (±7)][d]	6.82 (±0.29)[c]	−29 (±7) [−42 (±10)][d]
(*R*)-**6e**[f]	*p*-F-Ph	—	—	7.22 (±0.10)	25 (±3)
(*S*)-**6f**[f]	*m*-F-Ph	5.97 (±0.41)[c]	−30 (±9) [−41 (±12)][d]	7.37 (±0.17)[c]	−24 (±8) [−36 (±12)][d]
(*R*)-**6f**[f]	*m*-F-Ph	6.76 (±0.13)[c]	−43 (±4) [−59 (±5)][d]	8.62 (±0.29)[c]	−40 (±10) [−59 (±15)][d]
HU-308	—	7.76 (±0.11)	89 (±5)	7.40 (±0.03)	91 (±4)
SR-144,528[d]	—	5.56 (±0.13)[c]	−73 (±8) [−100 (±11)][d]	7.97 (±0.09)[c]	−68 (±4) [100 (±6)][d]
CP-55,940	—	9.11 (±0.07)	100 (±4)	8.52 (±0.03)	100 (±2)

[a] Potency (pEC_{50}) and efficacy (E_{max}) data were obtained in a cAMP HTRF assay using hCB_2R–CHO cells. [b] Potency (pEC_{50}) and E_{max} data were obtained in a G_i-CASE BRET-based assay using membrane preparations from hCB_2R-HEK293 T-REx cells. Data were normalized to agonist CP-55,940 response (100%) and basal level (0%). [c] Entries reflect pIC_{50}. [d] Data were additionally normalized to inverse agonist SR-144,528 (ref. 51) (100%) and basal level (0%) and are shown in brackets. Data shown as a mean (±SEM), N = 3–4. [e] C(2′) Diastereomeric mixture. [f] C(2′) Configuration assigned by analogy.

HEK293 T-REx cells that contain a genetically encoded fluorescence NanoLuciferase donor and Venus acceptor protein conjugated to the G_α and G_γ subunits, respectively, were co-incubated with the compounds and the Δ BRET signal was detected (Table 2). CB_2R activation by agonists leads to dissociation of the G_α and $G_{\beta\gamma}$ subunits, which in turn results in a reduction of BRET signal. Analogously, inverse agonists lead to an increase in BRET signal by G protein accumulation.

The G_i-CASE data follow the trends observed with functional data obtained from the HTRF cAMP assay (Table 2, solid blue line Fig. 3). Agonists (*R*)-**1** and (*S*)-**1** displayed comparable pEC_{50} values to the cAMP assay (6.48 and 9.42, respectively) with attenuated efficacy (E_{max} = 62 and 78%, respectively) compared to the HU-308 parent ligand (E_{max} = 91%). Interestingly, (*S*)-**1** displayed 100-fold increased potency relative to HU-308 (pEC_{50} = 7.40) in the assay. (*S*/*R*)-**6a** (E_{max} = 40%), (*S*)-**6c** (E_{max} = 80%), and (*S*/*R*)-**6c** (E_{max} = 67%) retained their partial agonist character in the G_i-CASE assay compared to the cAMP assay. However, in contrast to the cAMP functional readout as inverse agonist, (*S*/*R*)-**6b** displayed weak partial agonist properties (pEC_{50} = 7.15, E_{max} = 24%) in the G_i-CASE assay. We hypothesize that the ligands that show low efficacy may display protean behavior in terms of functionality across assays. Differences in the basal activity across assays or tissues may move partial agonists into the neutral antagonist/inverse agonist realm (and *vice versa*) – a known phenomenon for class A GPCRs.[33,68,69] Indeed, other protean ligands at CB_2R have been reported in the literature.[35,70–72] Additionally, specific conditions of the assays may exhibit a bias in terms of accessible receptor conformations because of the truncated or modified cannabinoid receptors employed.[49]

Ligands bearing aromatic sidechains (*S*)-**6d** (E_{max} = −28%), (*R*)-**6d** (E_{max} = −43%), (*S*)-**6e** (E_{max} = −29%), (*S*)-**6f** (E_{max} = −24%), and (*R*)-**6f** (E_{max} = −40%) corroborated the functional profiles established by the HTRF cAMP assay. Only the results for *para*-F substituted (*R*)-**6e** deviated from the trend (pEC_{50} = 7.22, E_{max} = 25%), suggesting that (*R*)-**6e** may act as protean agonists in a context dependent fashion. The compound's reduced affinity could be a driving factor behind its observed functionality.

Complementary assays reveal context-dependent function. We then turned our attention to further profile the identified agonists' and partial agonists' effects on β-arrestin recruitment, a further canonical and well-studied signaling pathway of CB_2R that is G protein independent.[73,74] To this end, we employed a BRET-based β-arrestin 2 (Arr2) recruitment assay. In parallel, we performed a mini-G_i recruitment assay to provide an additional, complementary G protein-based assay that is completely unamplified, measuring receptor–G_i association rather than heterotrimer dissociation. As the parent scaffold of our ligands, HU-308, is known to exhibit β-arrestin-biased signaling,[51] in contrast to the functionally unbiased profile of the balanced agonist CP-55,940, we were also interested to investigate if the bias of the parent scaffold would translate to its C(2′)-modified derivatives. Biased signaling in class A GPCRs[75] has been suggested to offer potential therapeutic advantages over balanced agonists due to their more focused signaling profile and has garnered significant attention in regard to CB_2R[51,76–78] as well as CB_1R for agonists with attenuated side effects.[79]

Notably, compounds (*S*/*R*)-**6a** and (*S*/*R*)-**6b** did not induce measurable recruitment of effector proteins in the β-arrestin as well as in the mini-G_i assay (Table 3). This lack of recruitment is consistent with their low efficacy and assay-dependent behavior observed in cAMP and G_i-CASE assays. (*S*)-**6c** and (*S*/*R*)-**6c**, more efficacious agonists in the previous assays, showed moderate potency and efficacy in the β-arrestin assay (pEC_{50} = 7.48, E_{max} = 41% and pEC_{50} = 7.91, E_{max} = 43%, respectively) as well as in the mini-G_i assay (pEC_{50} = 6.97, E_{max} = 51% and pEC_{50} = 7.40, E_{max} = 50%, respectively). Interestingly, while (*S*)-**1** displayed robust G_i and β-arrestin recruitment (pEC_{50} = 7.44, E_{max} = 86% and pEC_{50} = 7.12, E_{max} = 72%, respectively), (*R*)-**1** failed to elicit a response in both assays (mini-G_i and β-arrestin) and did not measurably recruit either effector protein. An observable trend for this set of essays is that only very efficacious agonists elicited

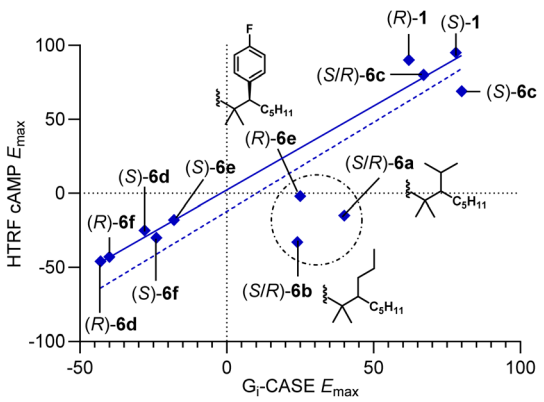

Fig. 3 Efficacy correlation between HTRF cAMP and G_i-CASE assays. Compounds enclosed within the circle (*S*/*R*)-**6a**, (*S*/*R*)-**6b**, and (*R*)-**6e** show protean behavior across the two assays. Solid blue line = correlation excluding compounds within the circle (R = 0.98). Dotted line = correlation including all compounds (R = 0.88). Data were normalized to agonist CP-55,940 response (100%) and basal level (0%).

Table 3 Functional characterization: mini-G_i Protein[a] and β-Arrestin recruitment[b] at CB_2R[c]

		Mini-G_i assay		β-arrestin assay	
Ligand	C(2′)-R	pEC_{50}	E_{max}/%	pEC_{50}	E_{max}/%
(*R*)-**1**	CF_3	—	—	—	—
(*S*)-**1**	CF_3	7.12 (±0.17)	72 (±5)	7.44 (±0.10)	86 (±4)
(*S*/*R*)-**6a**[d]	*i*-Pr	—	—	—	—
(*S*/*R*)-**6b**[d]	*n*-Pr	—	—	—	—
(*S*)-**6c**[e]	Et	6.97 (±0.07)	51 (±5)	7.48 (±0.20)	41 (±5)
(*S*/*R*)-**6c**[d]	Et	7.40 (±0.17)	50 (±2)	7.91 (±0.08)	43 (±3)
HU-308	—	6.93 (±0.11)	79 (±9)	7.07 (±0.10)	94 (±13)
CP-55,940	—	8.37 (±0.06)	100 (±1)	8.14 (±0.16)	100 (±2)

[a] Potency (pEC_{50}) and E_{max} data were obtained in a mini-G_i BRET-based assay using hCB_2R-HEK293 T-REx cells. [b] Potency (pEC_{50}) and E_{max} data were obtained in a β-arrestin BRET-based assay using hCB_2R-HEK293 T-REx cells. [c] Functional data were normalized to agonist CP-55,940 response (100%) and basal level (0%). Data shown as a mean (±SEM), N = 6–8. [d] C(2′) Diastereomeric mixture. [e] C(2′) Configuration assigned by analogy.

a response, suggesting that β-arrestin and mini-G_i assays are well-suited for comparative assessment for the profiling of efficacious ligands because of their unamplified and associative nature. Conversely, more sensitive assays such as G_i-CASE (lower receptor reserve)[66] and HTRF cAMP (downstream amplification) may be better suited for the identification of protean ligands.

Data from the compounds that were able to elicit a response in the mini-G_i and β-arrestin assays was furthermore used to assess whether the ligands showed biased signaling behavior according to the method developed by Bouvier and co-workers.[80] Indeed, (*S*)-**1**, (*S*)-**6c**, (*S*/*R*)-**6c** displayed bias towards β-arrestin signaling, mirroring the behavior of HU-308 (see SI Table S1 and Fig. S3). This suggests that C(2′) substitution has a limited impact on biased signaling and that the scaffold's preference for β-arrestin recruitment is governed by other structural determinants which are beyond the scope of this work.

Strategic modifications to HU-308 scaffold fine-tune signaling profile. In general, our results across different functional assays correlate. Exceptions include ligands showing protean behavior in terms of functionality: partial agonists that can also display neutral antagonist or moderate inverse agonist character (*i.e.* compounds (*R*)-**1**, (*R*)-**6e**, (*S*/*R*)-**6a**, and (*S*/*R*)-**6b**). We attribute this phenomenon to different basal activities and protein constructs across assays. As exemplified in the G_i-CASE assay, a generally identifiable trend for our HU-308 derivatives is that aryl groups at the C(2′) position induce a functionality switch from agonism to inverse agonism (Fig. 4). Based on our working model, we suggest that inactivation of the receptor occurs by steric interaction-driven reorientation of the toggle switch into the conformation that leads to stabilization of the inactive state of CB_2R. Fluorinated phenyls are tolerated, albeit at the cost of potency. The only exception to this trend of decreased potency is *meta*-F-substituted compound (*R*)-**6f**, which showed slightly increased potency (pEC_{50} = 8.62 *vs.* pEC_{50} = 8.47) compared to benchmark compound (*R*)-**6d** (Table 2). Alkyl substitution at the C(2′) position generally leads to partial agonists, with (*S*/*R*)-**6a** and (*S*/*R*)-**6b** displaying antagonist character in the mini-G_i and β-arrestin assays, presumably due to their low efficacy and the non-amplified character of these assays. Compound (*S*/*R*)-**6a** displayed inverse agonist properties in the cAMP assay, illustrating how low potency ligands have the potential to elicit a range of context-dependent functional outcomes.

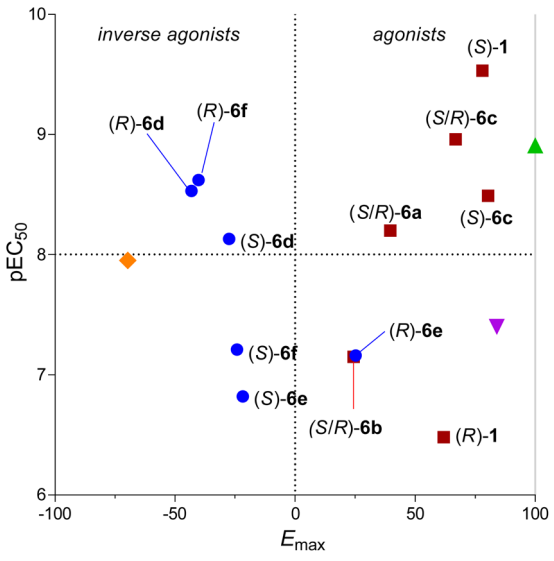

Fig. 4 Correlation diagram of ligand potency *vs.* efficacy as assessed in the G_i-CASE assay. (▼ = HU-308; ▲ = CP,55 940; ◆ = SR-144,528 ● = aryl substituent; ■ = alkyl substituent). Data were normalized to agonist CP-55,940 response (100%) and basal level (0%).

Of the compounds with C(2′) aliphatic substitution, (*S*)-**1** is an especially interesting case, as the introduction of a CF_3 residue leads to a significant increase in potency as well as efficacy compared to the parent compound HU-308 in the G_i-CASE assay. In contrast, diastereomer (*R*)-**1** displays a stark drop in affinity and potency at CB_2R and did not recruit effector proteins in the mini-G_i and β-arrestin assays.

Of note, although G_i-CASE, HTRF cAMP, and mini-G_i assays all probe G protein-coupled signaling, they can yield markedly different outcomes, particularly for ligands that do not act as full agonists. Evaluating ligands across multiple functional assays is important, particularly for G protein-coupled pathways of signaling, since results can vary depending on where in the signaling cascade the measurement is taken.[67] Context-dependency influenced by basal signaling tone as well as assay conditions and sensitivity can lead to functional profiles that may not be recapitulated across other assays targeting the same pathway. For instance, (*R*)-**1** did not significantly recruit mini-G_i but did act as a partial agonist in the G_i-CASE (E_{max} = 62%) and HTRF cAMP (E_{max} = 90%) assays. Our results are consistent with previous observations that show how narrow functional profiling may lead to premature identification of seemingly clear-cut functional profiles, highlighting the importance of early, thorough profiling across multiple and comparable assay platforms.[51]

Molecular dynamics investigation of (*R*)-1 and (*S*)-1

Given the distinct pharmacological profile of compounds (*R*)-**1** and (*S*)-**1**, as discussed above, molecular dynamics (MD) simulations were employed. We selected the X-ray structure of CB_2R in its inactive conformation (PDB: 5ZTY) as the starting point for the MD simulations in order to investigate ligand-induced transition toward the active state.[81,82] Starting from the inactive state rather than the active state is an approach to explore potential differences in receptor activation triggered by the two compounds (*R*)-**1** and (*S*)-**1**. Within the orthosteric binding site, both epimers are predicted to exhibit the previously reported, canonical HU-308 L-shaped conformation[40,49,50] which is stable over the simulated time of 1 μs (Fig. 5 and see SI). The hydroxyl group on the pinene core of both compounds (Fig. 5A for (*R*)-**1**, Fig. 5B for (*S*)-**1**) is predicted to form a hydrogen-bond with $His95^{2.65}$.

The structure of the CB_2R/(*R*)-**1** simulated complex reflects an inactive state of the receptor. Conversely, in the simulation, the CF_3 group of (*S*)-**1** engages the indole of $Trp258^{6.48}$ in a close

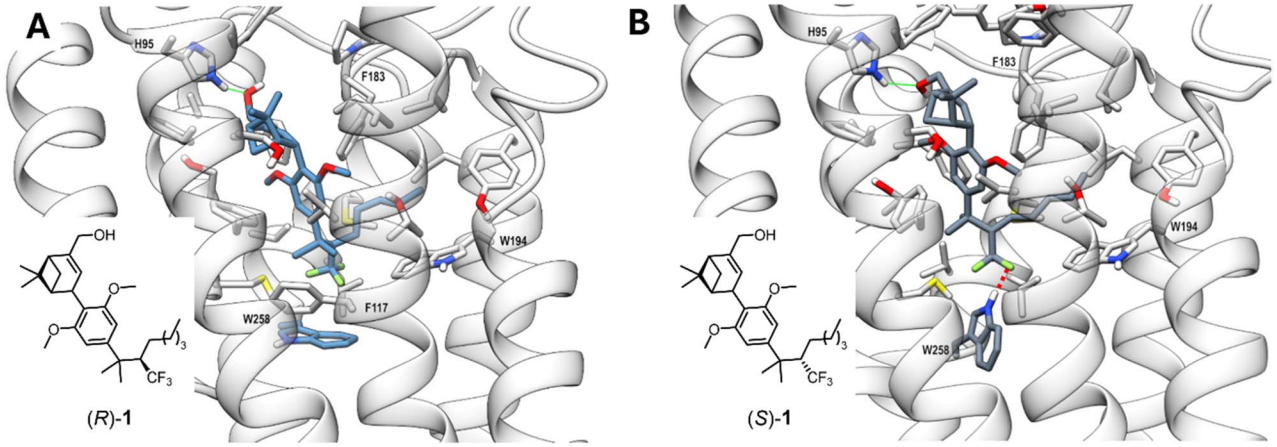

Fig. 5 Representative frames from MD simulations of CB_2R in complex with CF_3-bearing epimers (*R*)-**1** and (*S*)-**1**. (*R*)-**1** is colored in steel blue (A), (*S*)-**1** in slate gray (B). A stick representation is used for heavy atoms of the ligand and for protein sidechains within 5 Å of the ligand. Protein backbone atoms are represented as ribbons colored in light gray. Hydrogen, nitrogen, oxygen, and sulfur atoms are colored white, blue, red, and yellow, respectively. A green wire representation is adopted for peripheral H-bonds and a red dash representation for the key interaction in (B).

contact interaction that promotes a reorientation of the Trp258$^{6.48}$ sidechain. This interaction is reflected by a shorter distance between the fluorine atoms of (*S*)-**1** and the NE1 atom of Trp258$^{6.48}$ in the CB_2R/(*S*)-**1** complex (≤3.5 Å in 50.07% of the MD frames) compared to the CB_2R/(*R*)-**1** complex over the simulation period (see SI Fig. S5). Furthermore, only in the CB_2R/(*S*)-**1** simulated complex is the ionic lock (not shown in Fig. 5) between Arg131$^{3.50}$ and Asp240$^{6.30}$ disrupted, indicating a conformational shift towards the activated form of CB_2R (see SI Fig. S6).[40] Finally, the difference in free energy of binding ($\Delta\Delta G$) between the two epimers, obtained by performing molecular mechanics/Poisson–Boltzmann (Generalized Born) surface area (MM/PB(GB)SA), shows that (*S*)-**1** in complex is more stable by 3.55 kcal mol^{-1} (MM/GBSA) and 3.53 kcal mol^{-1} (MM/PBSA) than (*R*)-**1** (see SI), providing insight for the marked difference in affinity between the two compounds. Overall, the MD simulations suggest that (*S*)-**1** may demonstrate both higher receptor affinity and an agonist-like profile, providing a compelling rationale for its experimentally observed greater propensity for inducing CB_2R activation and a greater affinity for the receptor compared to (*R*)-**1**.

Conclusions

We have demonstrated that peripheral structural changes to an established agonist scaffold enable access to the entire efficacy spectrum at CB_2R. In line with our initial hypothesis that varying substituent size at the C(2′) position of HU-308-derived ligands would modulate the CB_2R toggle switch and thereby affect functional outcome, targeting the modulation of Trp258$^{6.48}$ enables graded functional outcomes. Our design considerations for reutilizing the canonical CB_2R ligand HU-308 were guided by a qualitative docking model that allowed for assessment of interaction with the toggle switch. Synthesis of a panel of designed ligands was achieved by a unified approach that required a modified HAT-reduction for access to CF_3-bearing derivatives. The ligands' subsequent pharmacological profiling revealed a wide range of accessible functionalities, from full agonists to partial agonists and neutral antagonists to inverse agonists. Notably, (*S*)-**1** showed high potency and β-arrestin bias, whereas its (*R*)-epimer exhibited reduced potency and failed to recruit effector proteins in both mini-G_i and β-arrestin assays. This exemplifies the marked impact that minor modifications, such as the introduction of a CF_3 group, can have on receptor binding affinity and functional outcomes. These findings were further substantiated by molecular dynamics simulations, which provided mechanistic insights into the proposed effect of a close-contact interaction with the toggle switch residue and its influence on the increased affinity and activity of (*S*)-**1** compared to (*R*)-**1** and HU-308.

Our study, exemplified by precision pharmacology at CB_2R, demonstrates how mechanistic understanding of class A GPCR activation facilitates rational design of fine-tunable ligands based on a single chemical scaffold and its binding modes in the orthosteric pocket. Derivatives with smaller aliphatic sidechains generally promote partial agonist activity that can switch into antagonist territory in a context-dependent manner. In contrast, sterically more demanding aromatic sidechains tend to induce inverse agonism or neutral antagonism, with those derivatives revealing a tight size tolerance for the cleft harboring the CB_2R single-residue toggle switch.

More broadly, this work underscores the potential of scaffold reutilization on the basis of rational ligand design to achieve functional outcomes at designated positions on the efficacy spectrum. The approach presented herein is possible because of diversity-oriented synthesis strategies that enable modification at C(2′) of the HU-308 scaffold. Traditional focused library synthesis leads to variety of structures aimed typically at optimizing for one outcome. The present approach leverages targeted structural diversification to access diversity across a range of functionality.

Reutilizing known GPCR ligand scaffolds in this manner may be useful for early-stage discovery by leveraging pre-existing pharmacological and synthetic knowledge. Designing class A

GPCR ligands that target toggle switches based on a single scaffold may provide a practical strategy to rapidly produce families of ligands with minimal modifications that display distinct functional profiles.

Author contributions

E. M. C., D. B. V., D. A. S., U. G. conceived and oversaw the project. M. K. and R. L. Z. G. conceived the project, conceived chemical experiments and synthetic routes to tool compounds and derivatives, synthesized compounds, and analyzed data of chemical synthesis as well as biological data. U. G. further provided project administration and logistics. Y. H. and T. P. P. performed selected biological assays (G_i-CASE). Y. H. performed data analysis and comparative data analysis on selected biological assays (G_i-CASE, HTRF cAMP). R. M. V. and P. A. performed the molecular dynamics (MD) simulations. T. H. conceived oversaw the performed HTRF cAMP assays. X. L. and Z. Z. performed HTRF cAMP assays and provided data analysis thereof. D. A. S. conceived and performed biological assays and provided data analysis thereof as well as resulting calculations (Tb-FRET, G_i-CASE, m-G_i, β-arrestin). W. G. conceived and oversaw the docking studies. K. A. and W. G. performed the docking studies. R. B., P. T., S. B., and C. B. conducted experiments and analytics pertaining to the attempted asymmetric hydrogenation. K. J. P., B. K., T. E. N. S., L. R., and U. G.-B. performed the synthesis of selected compounds. R. L. Z. G., M. K., and E. M. C. wrote the manuscript. All authors participated in discussion and preparation of the manuscript.

Conflicts of interest

The authors declare the following competing financial interest: M. K., B. K., W. G., U. G., and E. M. C. have filed a patent on CB_2R selective modulators and fluorescent probes.

Data availability

Experimental data associated with this work are available in the supplementary information (SI). Supplementary information is available. See DOI: https://doi.org/10.1039/d6sc00062b.

CCDC 2450722 contains the supplementary crystallographic data for this paper.[83]

Acknowledgements

We thank Eric Bald for his help with chiral separations and Isabelle Kaufmann for her assistance with logistics and administration. We are grateful to Dr Kurt Püntener and Manuela Müller for their expertise, insight, and experimental help with high-pressure hydrogenations. We thank René Arnold, Rainer Frankenstein, and Stephan Burkhardt for their help with NMR measurements, Jan Kovacovic for his expertise with high-pressure hydrogenation, and the MoBiAS team for MS analysis. We are grateful to Dr Nils Trapp and Michael Solar for X-ray crystallographic analysis. M. K. gratefully acknowledges a fellowship by the Scholarship Fund of the Swiss Chemical Industry (SSCI). T. H. was supported by the National Natural Science Foundation of China grant 32471267. MD studies were funded by project code PIR01_00011 "IBISCo", PON 2014–2020.

Notes and references

1 A. S. Hauser, S. Chavali, I. Masuho, L. J. Jahn, K. A. Martemyanov, D. E. Gloriam and M. M. Babu, Pharmacogenomics of GPCR Drug Targets, *Cell*, 2018, **172**, 41–54.
2 M. Zhang, T. Chen, X. Lu, X. Lan, Z. Chen and S. Lu, G protein-coupled receptors (GPCRs): advances in structures, mechanisms, and drug discovery, *Signal Transduction Targeted Ther.*, 2024, **9**, 88.
3 J. S. Lorente, A. V. Sokolov, G. Ferguson, H. B. Schioth, A. S. Hauser and D. E. Gloriam, GPCR drug discovery: new agents, targets and indications, *Nat. Rev. Drug Discovery*, 2025, **24**, 458–479.
4 D. Yang, Q. Zhou, V. Labroska, S. Qin, S. Darbalaei, Y. Wu, E. Yuliantie, L. Xie, H. Tao, J. Cheng, Q. Liu, S. Zhao, W. Shui, Y. Jiang and M. W. Wang, G protein-coupled receptors: structure- and function-based drug discovery, *Signal Transduction Targeted Ther.*, 2021, **6**, 7.
5 A. S. Hauser, M. M. Attwood, M. Rask-Andersen, H. B. Schioth and D. E. Gloriam, Trends in GPCR drug discovery: new agents, targets and indications, *Nat. Rev. Drug Discovery*, 2017, **16**, 829–842.
6 The Insight Partners 2023, *Small Molecule Drug Discovery Market Key Players and Opportunities by 2031*, https://www.theinsightpartners.com/reports/small-molecule-drug-discovery-market, accessed 18 Dec 2025.
7 P. Morales, M. M. Scharf, C. P. Johnson, A. Di Pizio and D. Hilger, Editorial: New approaches for the discovery of GPCR ligands, *Front. Endocrinol.*, 2023, **14**, 1272700.
8 O. J. Wouters, M. McKee and J. Luyten, Estimated Research and Development Investment Needed to Bring a New Medicine to Market, 2009-2018, *JAMA*, 2020, **323**, 844–853.
9 A. Sertkaya, T. Beleche, A. Jessup and B. D. Sommers, Costs of Drug Development and Research and Development Intensity in the US, 2000-2018, *JAMA Netw. Open*, 2024, **7**, e2415445.
10 S. M. Paul, D. S. Mytelka, C. T. Dunwiddie, C. C. Persinger, B. H. Munos, S. R. Lindborg and A. L. Schacht, How to improve R&D productivity: the pharmaceutical industry's grand challenge, *Nat. Rev. Drug Discovery*, 2010, **9**, 203–214.
11 P. Addis, U. Bali, F. Baron, A. Campbell, S. Harborne, L. Jagger, G. Milne, M. Pearce, E. M. Rosethorne, R. Satchell, D. Swift, B. Young and J. F. Unitt, Key aspects of modern GPCR drug discovery, *SLAS Discovery*, 2024, **29**, 1–22.
12 M. Maccarrone, V. Di Marzo, J. Gertsch, U. Grether, A. C. Howlett, T. Hua, A. Makriyannis, D. Piomelli, N. Ueda and M. van der Stelt, Goods and Bads of the Endocannabinoid System as a Therapeutic Target: Lessons Learned after 30 Years, *Pharmacol. Rev.*, 2023, **75**, 885–958.

13 F. Shahbazi, V. Grandi, A. Banerjee and J. F. Trant, Cannabinoids and Cannabinoid Receptors: The Story so Far, *iScience*, 2020, **23**, 101301.
14 S. Galiegue, S. Mary, J. Marchand, D. Dussossoy, D. Carriere, P. Carayon, M. Bouaboula, D. Shire, G. Le Fur and P. Casellas, Expression of central and peripheral cannabinoid receptors in human immune tissues and leukocyte subpopulations, *Eur. J. Biochem.*, 1995, **232**, 54–61.
15 P. Pacher and R. Mechoulam, Is lipid signaling through cannabinoid 2 receptors part of a protective system?, *Prog. Lipid Res.*, 2011, **50**, 193–211.
16 K. Bala, P. Porel and K. R. Aran, Emerging roles of cannabinoid receptor CB2 receptor in the central nervous system: therapeutic target for CNS disorders, *Psychopharmacology*, 2024, **241**, 1939–1954.
17 E. D. Goncalves and R. C. Dutra, Cannabinoid receptors as therapeutic targets for autoimmune diseases: where do we stand?, *Drug Discovery Today*, 2019, **24**, 1845–1853.
18 H. Khan, F. K. Ghori, U. Ghani, A. Javed and S. Zahid, Cannabinoid and endocannabinoid system: a promising therapeutic intervention for multiple sclerosis, *Mol. Biol. Rep.*, 2022, **49**, 5117–5131.
19 N. J. van den Hoogen, E. K. Harding, C. E. D. Davidson and T. Trang, Cannabinoids in Chronic Pain: Therapeutic Potential Through Microglia Modulation, *Front. Neural Circuits*, 2021, **15**, 816747.
20 Y. Shang and Y. Tang, The central cannabinoid receptor type-2 (CB2) and chronic pain, *Int. J. Neurosci.*, 2017, **127**, 812–823.
21 C. Laezza, C. Pagano, G. Navarra, O. Pastorino, M. C. Proto, D. Fiore, C. Piscopo, P. Gazzerro and M. Bifulco, The Endocannabinoid System: A Target for Cancer Treatment, *Int. J. Mol. Sci.*, 2020, **21**, 747–767.
22 M. B. Faiz, F. Naeem, M. Irfan, M. A. Aslam, L. M. Estevinho, D. A. Atessahin, A. M. Alshahrani, D. Calina, K. Khan and J. Sharifi-Rad, Exploring the therapeutic potential of cannabinoids in cancer by modulating signaling pathways and addressing clinical challenges, *Discover Oncol.*, 2024, **15**, 490.
23 F. A. Moreira, M. Grieb and B. Lutz, Central side-effects of therapies based on CB1 cannabinoid receptor agonists and antagonists: focus on anxiety and depression, *Best Pract. Res., Clin. Endocrinol. Metab.*, 2009, **23**, 133–144.
24 J. L. Wilkerson, J. A. Bilbrey, J. S. Felix, A. Makriyannis and L. R. McMahon, Untapped endocannabinoid pharmacological targets: Pipe dream or pipeline?, *Pharmacol., Biochem. Behav.*, 2021, **206**, 173192.
25 M. Kosar, L. Mach, E. M. Carreira, M. Nazare, P. Pacher and U. Grether, Patent review of cannabinoid receptor type 2 (CB(2)R) modulators (2016-present), *Expert Opin. Ther. Pat.*, 2024, **34**, 665–700.
26 TT-816 As Monotherapy or in Combination with a PD-1 Inhibitor in Patients with Advanced Cancers (SEABEAM) (MK3475-E88), https://clinicaltrials.gov/study/NCT05525455, accessed 4. Jan 2025.
27 Olorinab in Irritable Bowel Syndrome With Predominant Constipation (IBS-C) and Irritable Bowel Syndrome With Predominant Diarrhea (IBS-D) (CAPTIVATE), https://clinicaltrials.gov/study/NCT04043455, accessed 4. Jan 2025.
28 Corbus Pharmaceuticals – Lenabasum, https://adisinsight.springer.com/drugs/800007180, accessed 4. Jan 2026.
29 R. Ganzoni, Figure created in BioRender, 2025, Figure_1_part1: https://BioRender.com/m8n0bwm; Figure_1_part2: https://BioRender.com/gak69nf; TOC: https://BioRender.com/vbn1xif.
30 P. Mukhopadhyay, M. Baggelaar, K. Erdelyi, Z. Cao, R. Cinar, F. Fezza, B. Ignatowska-Janlowska, J. Wilkerson, N. van Gils, T. Hansen, M. Ruben, M. Soethoudt, L. Heitman, G. Kunos, M. Maccarrone, A. Lichtman, P. Pacher and M. Van der Stelt, The novel, orally available and peripherally restricted selective cannabinoid CB2 receptor agonist LEI-101 prevents cisplatin-induced nephrotoxicity, *Br. J. Pharmacol.*, 2016, **173**, 446–458.
31 A. I. Uba, H. Aluwala, H. Liu and C. Wu, Elucidation of partial activation of cannabinoid receptor type 2 and identification of potential partial agonists: Molecular dynamics simulation and structure-based virtual screening, *Comput. Biol. Chem.*, 2022, **99**, 107723.
32 K. J. Valenzano, L. Tafesse, G. Lee, J. E. Harrison, J. M. Boulet, S. L. Gottshall, L. Mark, M. S. Pearson, W. Miller, S. Shan, L. Rabadi, Y. Rotshteyn, S. M. Chaffer, P. I. Turchin, D. A. Elsemore, M. Toth, L. Koetzner and G. T. Whiteside, Pharmacological and pharmacokinetic characterization of the cannabinoid receptor 2 agonist, GW405833, utilizing rodent models of acute and chronic pain, anxiety, ataxia and catalepsy, *Neuropharmacology*, 2005, **48**, 658–672.
33 H. Kurose and S. G. Kim, Pharmacology of Antagonism of GPCR, *Biol. Pharm. Bull.*, 2022, **45**, 669–674.
34 T. Kenakin, Efficacy at G-protein-coupled receptors, *Nat. Rev. Drug Discovery*, 2002, **1**, 103–110.
35 I. Mancini, R. Brusa, G. Quadrato, C. Foglia, P. Scandroglio, L. S. Silverman, D. Tulshian, A. Reggiani and M. Beltramo, Constitutive activity of cannabinoid-2 (CB2) receptors plays an essential role in the protean agonism of (+)AM1241 and L768242, *Br. J. Pharmacol.*, 2009, **158**, 382–391.
36 M. Wu, E. Carballo-Jane, H. Zhou, P. Zafian, G. Dai, M. Liu, J. Lao, T. Kelly, D. Shao, J. Gorski, D. Pissarnitski, A. Kekec, Y. Chen, S. F. Previs, G. Scapin, Y. Gomez-Llorente, S. A. Hollingsworth, L. Yan, D. Feng, P. Huo, G. Walford, M. D. Erion, D. E. Kelley, S. Lin and J. Mu, Functionally selective signaling and broad metabolic benefits by novel insulin receptor partial agonists, *Nat. Commun.*, 2022, **13**, 942.
37 R. I. Ohlsen and L. S. Pilowsky, The place of partial agonism in psychiatry: recent developments, *J. Psychopharmacol.*, 2005, **19**, 408–413.
38 E. L. Theunissen, K. P. C. Kuypers, N. L. Mason and J. G. Ramaekers, A Comparison of Acute Neurocognitive and Psychotomimetic Effects of a Synthetic Cannabinoid and Natural Cannabis at Psychotropic Dose Equivalence, *Front. Psychiatry.*, 2022, **13**, 891811.
39 T. S. Thorsen, Y. Kulkarni, D. A. Sykes, A. Boggild, T. Drace, P. Hompluem, C. Iliopoulos-Tsoutsouvas, S. P. Nikas,

H. Daver, A. Makriyannis, P. Nissen, M. Gajhede, D. B. Veprintsev, T. Boesen, J. S. Kastrup and D. E. Gloriam, Structural basis of THC analog activity at the Cannabinoid 1 receptor, *Nat. Commun.*, 2025, **16**, 486.

40 X. Li, H. Chang, J. Bouma, L. V. de Paus, P. Mukhopadhyay, J. Paloczi, M. Mustafa, C. van der Horst, S. S. Kumar, L. Wu, Y. Yu, R. van den Berg, A. P. A. Janssen, A. Lichtman, Z. J. Liu, P. Pacher, M. van der Stelt, L. H. Heitman and T. Hua, Structural basis of selective cannabinoid CB(2) receptor activation, *Nat. Commun.*, 2023, **14**, 1447.

41 B. Csoka, Z. H. Nemeth, P. Mukhopadhyay, Z. Spolarics, M. Rajesh, S. Federici, E. A. Deitch, S. Batkai, P. Pacher and G. Hasko, CB2 cannabinoid receptors contribute to bacterial invasion and mortality in polymicrobial sepsis, *PLoS One*, 2009, **4**, e6409.

42 J. Chen, F. Wang, S. Zhang, Q. Lin, H. Xu, T. Zhu, L. Peng, F. Cen, F. Li, Z. Wang, C. G. Feng, Z. Yin, Y. Liu and G. Zhang, Activation of CD4(+) T Cell-Derived Cannabinoid Receptor 2 Signaling Exacerbates Sepsis via Inhibiting IL-10, *J. Immunol.*, 2022, **208**, 2515–2522.

43 L. M. Wingler and R. J. Lefkowitz, Conformational Basis of G Protein-Coupled Receptor Signaling Versatility, *Trends Cell Biol.*, 2020, **30**, 736–747.

44 R. A. de Ligt, A. P. Kourounakis and I. J. AP, Inverse agonism at G protein-coupled receptors: (patho)physiological relevance and implications for drug discovery, *Br. J. Pharmacol.*, 2000, **130**, 1–12.

45 M. Kosar, R. C. Sarott, D. A. Sykes, A. E. G. Viray, R. M. Vitale, N. Tomasevic, X. Li, R. L. Z. Ganzoni, B. Kicin, L. Reichert, K. J. Patej, U. Gomez-Bouzo, W. Guba, P. J. McCormick, T. Hua, C. W. Gruber, D. B. Veprintsev, J. A. Frank, U. Grether and E. M. Carreira, Flipping the GPCR Switch: Structure-Based Development of Selective Cannabinoid Receptor 2 Inverse Agonists, *ACS Cent. Sci.*, 2024, **10**, 956–968.

46 L. Hanus, A. Breuer, S. Tchilibon, S. Shiloah, D. Goldenberg, M. Horowitz, R. G. Pertwee, R. A. Ross, R. Mechoulam and E. Fride, HU-308: a specific agonist for CB(2), a peripheral cannabinoid receptor, *Proc. Natl. Acad. Sci. U. S. A.*, 1999, **96**, 14228–14233.

47 X. Wang, C. Neale, S. K. Kim, W. A. Goddard and L. Ye, Intermediate-state-trapped mutants pinpoint G protein-coupled receptor conformational allostery, *Nat. Commun.*, 2023, **14**, 1325.

48 S. Filipek, Molecular switches in GPCRs, *Curr. Opin. Struct. Biol.*, 2019, **55**, 114–120.

49 X. Li, T. Hua, K. Vemuri, J. H. Ho, Y. Wu, L. Wu, P. Popov, O. Benchama, N. Zvonok, K. Locke, L. Qu, G. W. Han, M. R. Iyer, R. Cinar, N. J. Coffey, J. Wang, M. Wu, V. Katritch, S. Zhao, G. Kunos, L. M. Bohn, A. Makriyannis, R. C. Stevens and Z. J. Liu, Crystal Structure of the Human Cannabinoid Receptor CB2, *Cell*, 2019, **176**, 459–467.

50 T. Hua, X. Li, L. Wu, C. Iliopoulos-Tsoutsouvas, Y. Wang, M. Wu, L. Shen, C. A. Brust, S. P. Nikas, F. Song, X. Song, S. Yuan, Q. Sun, Y. Wu, S. Jiang, T. W. Grim, O. Benchama, E. L. Stahl, N. Zvonok, S. Zhao, L. M. Bohn, A. Makriyannis and Z. J. Liu, Activation and Signaling Mechanism Revealed by Cannabinoid Receptor-Gi Complex Structures, *Cell*, 2020, **180**, 655–665.

51 M. Soethoudt, U. Grether, J. Fingerle, T. W. Grim, F. Fezza, L. de Petrocellis, C. Ullmer, B. Rothenhausler, C. Perret, N. van Gils, D. Finlay, C. MacDonald, A. Chicca, M. D. Gens, J. Stuart, H. de Vries, N. Mastrangelo, L. Xia, G. Alachouzos, M. P. Baggelaar, A. Martella, E. D. Mock, H. Deng, L. H. Heitman, M. Connor, V. Di Marzo, J. Gertsch, A. H. Lichtman, M. Maccarrone, P. Pacher, M. Glass and M. van der Stelt, Cannabinoid CB(2) receptor ligand profiling reveals biased signalling and off-target activity, *Nat. Commun.*, 2017, **8**, 13958.

52 W. A. Devane, F. A. Dysarz 3rd, M. R. Johnson, L. S. Melvin and A. C. Howlett, Determination and characterization of a cannabinoid receptor in rat brain, *Mol. Pharmacol.*, 1988, **34**, 605–613.

53 M. Herkenham, A. B. Lynn, M. D. Little, M. R. Johnson, L. S. Melvin, B. R. de Costa and K. C. Rice, Cannabinoid receptor localization in brain, *Proc. Natl. Acad. Sci. U. S. A.*, 1990, **87**, 1932–1936.

54 J. W. Huffman, S. M. Bushell, S. N. Joshi, J. L. Wiley and B. R. Martin, Enantioselective synthesis of 1-methoxy- and 1-deoxy-2'-methyl-delta8-tetrahydrocannabinols: new selective ligands for the CB2 receptor, *Bioorg. Med. Chem.*, 2006, **14**, 247–262.

55 I. Ruppert, K. Schlich and W. Volbach, Die ersten CF3-substituierten organyl(chlor)silane, *Tetrahedron Lett.*, 1984, **25**, 2195–2198.

56 G. K. S. Prakash, R. Krishnamurti and G. A. Olah, Synthetic methods and reactions. 141. Fluoride-induced trifluoromethylation of carbonyl compounds with trifluoromethyltrimethylsilane (TMS-CF3). A trifluoromethide equivalent, *J. Am. Chem. Soc.*, 1989, **111**, 393–395.

57 V. Grignard, Mixed organomagnesium combinations and their application in acid, alcohol, and hydrocarbon synthesis, *Ann. Chim.*, 1901, **24**, 433–490.

58 M. S. Kharasch and S. Weinhouse, Grignard Reagents – their Reducing Action and Rates of Addition, *J. Org. Chem.*, 1936, **01**, 209–230.

59 K. Iwasaki, K. K. Wan, A. Oppedisano, S. W. Crossley and R. A. Shenvi, Simple, chemoselective hydrogenation with thermodynamic stereocontrol, *J. Am. Chem. Soc.*, 2014, **136**, 1300–1303.

60 A. Krasovskiy, F. Kopp and P. Knochel, Soluble lanthanide salts (LnCl3.2LiCl) for the improved addition of organomagnesium reagents to carbonyl compounds, *Angew Chem. Int. Ed. Engl.*, 2006, **45**, 497–500.

61 M. Kosar, D. A. Sykes, A. E. G. Viray, R. M. Vitale, R. C. Sarott, R. L. Ganzoni, D. Onion, J. M. Tobias, P. Leippe, C. Ullmer, E. A. Zirwes, W. Guba, U. Grether, J. A. Frank, D. B. Veprintsev and E. M. Carreira, Platform Reagents Enable Synthesis of Ligand-Directed Covalent Probes: Study of Cannabinoid Receptor 2 in Live Cells, *J. Am. Chem. Soc.*, 2023, **145**, 15094–15108.

62 R. C. Sarott, A. E. G. Viray, P. Pfaff, A. Sadybekov, G. Rajic, V. Katritch, E. M. Carreira and J. A. Frank, Optical Control

of Cannabinoid Receptor 2-Mediated Ca(2+) Release Enabled by Synthesis of Photoswitchable Probes, *J. Am. Chem. Soc.*, 2021, **143**, 736–743.

63 R. C. Sarott, M. V. Westphal, P. Pfaff, C. Korn, D. A. Sykes, T. Gazzi, B. Brennecke, K. Atz, M. Weise, Y. Mostinski, P. Hompluem, E. Koers, T. Miljus, N. J. Roth, H. Asmelash, M. C. Vong, J. Piovesan, W. Guba, A. C. Rufer, E. A. Kusznir, S. Huber, C. Raposo, E. A. Zirwes, A. Osterwald, A. Pavlovic, S. Moes, J. Beck, I. Benito-Cuesta, T. Grande, N. E. S. Ruiz de Marti, A. Yeliseev, F. Drawnel, G. Widmer, D. Holzer, T. van der Wel, H. Mandhair, C. Y. Yuan, W. R. Drobyski, Y. Saroz, N. Grimsey, M. Honer, J. Fingerle, K. Gawrisch, J. Romero, C. J. Hillard, Z. V. Varga, M. van der Stelt, P. Pacher, J. Gertsch, P. J. McCormick, C. Ullmer, S. Oddi, M. Maccarrone, D. B. Veprintsev, M. Nazare, U. Grether and E. M. Carreira, Development of High-Specificity Fluorescent Probes to Enable Cannabinoid Type 2 Receptor Studies in Living Cells, *J. Am. Chem. Soc.*, 2020, **142**, 16953–16964.

64 L. Borrega-Roman, B. L. Hoare, M. Kosar, R. C. Sarott, K. J. Patej, J. Bouma, M. Scott-Dennis, E. J. Koers, T. Gazzi, L. Mach, S. Barrondo, J. Salles, W. Guba, E. Kusznir, M. Nazare, A. C. Rufer, U. Grether, L. H. Heitman, E. M. Carreira, D. A. Sykes and D. B. Veprintsev, A universal cannabinoid CB1 and CB2 receptor TR-FRET kinetic ligand-binding assay, *Front. Pharmacol*, 2025, **16**, 1469986.

65 G. Wolfgang, M. Nazare and U. Grether, in *New Tools to Interrogate Endocannabinoid Signalling: From Natural Compounds to Synthetic Drugs*, ed. M. Maccarrone, The Royal Society of Chemistry, 2021, pp. 89–167, DOI: 10.1039/9781839160752.

66 M. Scott-Dennis, F. A. Rafani, Y. Yi, T. Perera, C. R. Harwood, W. Guba, A. C. Rufer, U. Grether, D. B. Veprintsev and D. A. Sykes, Development of a membrane-based Gi-CASE biosensor assay for profiling compounds at cannabinoid receptors, *Front. Pharmacol*, 2023, **14**, 1158091.

67 W. Stallaert, A. Christopoulos and M. Bouvier, Ligand functional selectivity and quantitative pharmacology at G protein-coupled receptors, *Expert Opin. Drug Discovery*, 2011, **6**, 811–825.

68 F. Gbahou, A. Rouleau, S. Morisset, R. Parmentier, S. Crochet, J. S. Lin, X. Ligneau, J. Tardivel-Lacombe, H. Stark, W. Schunack, C. R. Ganellin, J. C. Schwartz and J. M. Arrang, Protean agonism at histamine H3 receptors in vitro and in vivo, *Proc. Natl. Acad. Sci. U. S. A.*, 2003, **100**, 11086–11091.

69 J. McDonald, T. A. Barnes, H. Okawa, J. Williams, G. Calo, D. J. Rowbotham and D. G. Lambert, Partial agonist behaviour depends upon the level of nociceptin/orphanin FQ receptor expression: studies using the ecdysone-inducible mammalian expression system, *Br. J. Pharmacol.*, 2003, **140**, 61–70.

70 B. B. Yao, S. Mukherjee, Y. Fan, T. R. Garrison, A. V. Daza, G. K. Grayson, B. A. Hooker, M. J. Dart, J. P. Sullivan and M. D. Meyer, In vitro pharmacological characterization of AM1241: a protean agonist at the cannabinoid CB2 receptor?, *Br. J. Pharmacol.*, 2006, **149**, 145–154.

71 B. Bosier and E. Hermans, Versatility of GPCR recognition by drugs: from biological implications to therapeutic relevance, *Trends Pharmacol. Sci.*, 2007, **28**, 438–446.

72 B. Bosier, G. G. Muccioli, E. Hermans and D. M. Lambert, Functionally selective cannabinoid receptor signalling: therapeutic implications and opportunities, *Biochem. Pharmacol.*, 2010, **80**, 1–12.

73 Y. K. Peterson and L. M. Luttrell, The Diverse Roles of Arrestin Scaffolds in G Protein-Coupled Receptor Signaling, *Pharmacol. Rev.*, 2017, **69**, 256–297.

74 M. Patel, C. Matti, N. L. Grimsey, D. F. Legler, J. A. Javitch, D. B. Finlay and M. Glass, Delineating the interactions between the cannabinoid CB(2) receptor and its regulatory effectors; beta-arrestins and GPCR kinases, *Br. J. Pharmacol.*, 2022, **179**, 2223–2239.

75 P. Morales, M. M. Scharf, M. Bermudez, A. Egyed, R. Franco, O. K. Hansen, N. Jagerovic, J. Jakubik, G. M. Keseru, D. J. Kiss, P. Kozielewicz, O. Larsen, M. Majellaro, A. Mallo-Abreu, G. Navarro, R. Prieto-Diaz, M. M. Rosenkilde, E. Sotelo, H. Stark, T. Werner and L. M. Wingler, Progress on the development of Class A GPCR-biased ligands, *Br. J. Pharmacol.*, 2024, **182**, 3249–3300.

76 M. S. Ibsen, M. Connor and M. Glass, Cannabinoid CB(1) and CB(2) Receptor Signaling and Bias, *Cannabis Cannabinoid Res.*, 2017, **2**, 48–60.

77 E. Wouters, J. Walraed, S. D. Banister and C. P. Stove, Insights into biased signaling at cannabinoid receptors: synthetic cannabinoid receptor agonists, *Biochem. Pharmacol.*, 2019, **169**, 113623.

78 M. Patel, N. L. Grimsey, S. D. Banister, D. B. Finlay and M. Glass, Evaluating signaling bias for synthetic cannabinoid receptor agonists at the cannabinoid CB(2) receptor, *Pharmacol. Res. Perspect.*, 2023, **11**, e01157.

79 T. A. Tummino, C. Iliopoulos-Tsoutsouvas, J. M. Braz, E. S. O'Brien, R. M. Stein, V. Craik, N. K. Tran, S. Ganapathy, F. Liu, Y. Shiimura, F. Tong, T. C. Ho, D. S. Radchenko, Y. S. Moroz, S. R. Rosado, K. Bhardwaj, J. Benitez, Y. Liu, H. Kandasamy, C. Normand, M. Semache, L. Sabbagh, I. Glenn, J. J. Irwin, K. K. Kumar, A. Makriyannis, A. I. Basbaum and B. K. Shoichet, Virtual library docking for cannabinoid-1 receptor agonists with reduced side effects, *Nat. Commun.*, 2025, **16**, 2237.

80 E. T. van der Westhuizen, B. Breton, A. Christopoulos and M. Bouvier, Quantification of ligand bias for clinically relevant beta2-adrenergic receptor ligands: implications for drug taxonomy, *Mol. Pharmacol.*, 2014, **85**, 492–509.

81 W. I. Weis and B. K. Kobilka, The Molecular Basis of G Protein-Coupled Receptor Activation, *Annu. Rev. Biochem.*, 2018, **87**, 897–919.

82 O. Diaz, J. A. R. Dalton and J. Giraldo, Revealing the Mechanism of Agonist-Mediated Cannabinoid Receptor 1 (CB1) Activation and Phospholipid-Mediated Allosteric Modulation, *J. Med. Chem.*, 2019, **62**, 5638–5654.

83 CCDC 2450722: Experimental Crystal Structure Determination, 2026, DOI: 10.5517/ccdc.csd.cc2n85kp.